PHYSICAL REVIEW D **96,** 055041 (2017)

Radiative decays of a singlet scalar boson through vectorlike quarks

Yeo Woong Yoon,[1,*] Kingman Cheung,[1,2,3,†] Sin Kyu Kang,[4,‡] and Jeonghyeon Song[1,§]

[1]*School of Physics, KonKuk University, Seoul 05029, Korea*
[2]*Department of Physics, National Tsing Hua University, Hsinchu 300, Taiwan*
[3]*Physics Division, National Center for Theoretical Sciences, Hsinchu 300, Taiwan*
[4]*School of Liberal Arts, Seoul-Tech, Seoul 01811, Korea*

(Received 22 May 2017; published 27 September 2017)

If the standard model Higgs boson were much heavier, it would appear as a broad resonance since its decay into a pair of longitudinally polarized gauge bosons is highly enhanced. We study whether the same enhancement happens at loop level in a simple extension of the standard model with a singlet scalar boson S and three vectorlike quark multiplets. In order to focus on the loop effects, we assume that S does not interact with the standard model particles at tree level. Vectorlike quarks running in the loop link the singlet scalar S to the standard model world. There are two kinds of loop effects in the S phenomenology—the mixing with the Higgs boson and the radiative decays into hh, WW, ZZ, gg, and $\gamma\gamma$. We show that the crucial conditions for the loop-induced longitudinal polarization enhancement are the large mass differences among vectorlike quarks. The current LHC constraints from the heavy scalar searches and the Higgs precision data are shown to be very significant: the mixing angle with the Higgs boson should be smaller than about 0.1 for $m_S = 750$ GeV.

DOI: 10.1103/PhysRevD.96.055041

I. INTRODUCTION

The standard model (SM) has been more solidified by the Large Hadron Collider (LHC) data at $\sqrt{s} = 13$ TeV. Supersymmetry models, composite Higgs models, and other SM extensions are all strongly constrained. Despite the absence of new signals, we believe that new physics beyond the SM must exist since the issue of naturalness and the existence of dark matter cannot be explained within the SM. There are two kinds of strategies for no new signals, pushing new particles out of the LHC reach [1] or introducing a hidden sector [2,3]. If either is the case, we turn to radiative corrections mediated by new particles or the linking to the hidden sector [4].

An interesting question is how significantly the radiative correction or the linking changes tree-level results. They generally cause subleading corrections, but there exist extreme cases also. We may see entirely new signals which are absent at tree level, such as the flavor changing neutral current processes through loops and the invisible Higgs decay modes through the mixing with a hidden sector. In this work, we investigate a possibility that loop-induced new signals are so significant that they could be useful in the search for a new heavy scalar boson.

At tree level, the decay of a *heavy* scalar boson shows an intriguing and unique feature, the longitudinal polarization enhancement in its decay into a massive gauge boson pair. It is well-known that if the SM Higgs boson h were much heavier, it would have decayed dominantly into a heavy gauge boson pair, VV ($V = W, Z$). The $t\bar{t}$ channel, the next dominant one, has the maximum branching ratio about 19%. The extraordinarily large $\Gamma(h \to VV)$ when $m_h \gg m_V$ is due to its decay into the longitudinal modes, $V_L V_L$ [5,6]. The longitudinal polarization vector of V is proportional to p_V^μ / m_V in the high energy limit, which leads to $\Gamma(h \to V_L V_L) \propto m_h^3$. The heavier the Higgs boson is, the larger the decay rate into $V_L V_L$ becomes. For instance, $\Gamma(h \to V_L V_L)$ is about 99% of $\Gamma(h \to VV)$ when $m_h \simeq 440$ GeV. Accordingly its total decay rate is also enhanced so that a heavy Higgs boson becomes a broad resonance.

We wonder whether the same thing happens when a new heavy scalar boson decays *only radiatively*. To answer this question, we consider a simple extension of the SM with a singlet scalar S [7] and vectorlike quarks (VLQs) [8]. Recently, a singlet scalar has drawn a lot of interest. In the context of Higgs portal models, the singlet scalar serves as a mediator between the visible sector and the dark sector [2], or it can play the role of dark matter itself under some discrete symmetries. The phenomenological signatures in this direction have been extensively studied [9–15]. Another direction is in regard to the electroweak baryogenesis (EWBG) [16]. Successful EWBG requires strong first order phase transition of the electroweak symmetry breaking, which cannot occur in the SM Higgs sector due to the observed heavy Higgs boson mass [17]. With a new scalar S, the scalar field space is extended to accommodate the strong first order phase transition [18–25]. More interestingly, strong first order electroweak phase transition

*ywyoon@kias.re.kr
†kingman8cheung@gmail.com
‡skkang@snut.ac.kr
§jeonghyeon.song@gmail.com

in the early Universe has recently gotten a new window—the gravitation wave which was generated from the formation of bubbles of the broken phase [26–39].

Heavy VLQs are also inviting as they appear in many new physics models [40,41] such as composite Higgs models [42,43], extra dimension models [44,45], little Higgs models [46–48], and SUSY models [49–52]. The vectorlike nature makes the new heavy quarks easily allowed by the current experimental results: if chiral, they are excluded by the measurement of Higgs production rates [53–55]; the T parameter from the electroweak precision data is compatible with sizable mass differences among different VLQs [56]. We take special note that the *combination* of a singlet scalar and vectorlike quarks has many interesting features: it can shift the metastability of the electroweak vacuum in the SM [57–61]; it is crucial to construct a model where all of the gauge and Yukawa couplings remain asymptotically safe up to infinite energy [62,63]; it can accommodate the EWBG [64].

Considering all of the attractive merits, a new physics model with a singlet scalar and VLQs is well-motivated. We are content with a simplified model with focus on the singlet scalar and the VLQs without mentioning the UV completion. In addition, our driving question, whether the longitudinal polarization enhancement in $S\to WW/ZZ$ can be radiatively generated, is efficiently addressed in a limiting scenario of this model where S does not couple to the SM particles at tree level. The VLQs play the role of messengers as connecting the SM particles and S at loop level, as interacting with the singlet scalar S, the SM Higgs boson, and the SM gauge bosons. In order to allow the Yukawa interactions of VLQs with the Higgs boson, we introduce three VLQ multiplets, an $SU(2)_L$ doublet, and two (up-type and down-type) $SU(2)_L$ singlets. The presence of multiple VLQs shall be shown crucial in the S phenomenology. The VLQ loops have two kinds of implications. First S decays into gg, $\gamma\gamma$, WW, ZZ, and hh through triangle VLQ loops. The singlet scalar S can be produced and probed at high energy colliders. Secondly, S is radiatively mixed with the Higgs boson. Naive expectation is that the heavier the VLQs are, the smaller the loop corrections become. We shall show that this is not true. Large mass differences in the VLQ mass spectrum induce the longitudinal polarization enhancement and increase the S-h radiative mixing. The obtained condition for the enhancement at loop level shall help to study the physical properties of new particles running in the loop. These are our main results.

The paper is organized as follows. In Sec. II, we provide the general helicity amplitude framework for the decay of a scalar boson into a massive gauge boson pair and into a Higgs boson pair. Section III summarizes our new physics model with a singlet scalar S and VLQs. The gauge and Yukawa couplings of the VLQs in terms of the mass eigenstates are given. In Sec. IV, we present our main analytic results of loop calculations. The radiatively generated S-h mixing and the loop-induced decay rates of $S\to hh, VV$ are to be shown. In particular, the asymptotic behaviors of the loop functions are very useful to understand the enhancement of $\Gamma(S\to hh, VV)$ by large mass differences of the VLQs. Section V is devoted to our numerical results in a simple benchmark scenario. The general physical properties of S such as its branching ratio and total decay rate are studied. We also calculate the exclusion limits from the current LHC results of the heavy scalar searches and the Higgs precision observation. The future prospect at the 13 TeV LHC is also discussed. Section VI contains our conclusions.

II. DECAYS OF A SCALAR BOSON INTO VV AND hh

We consider a $\mathcal{J}^{\mathcal{PC}}=0^{++}$ scalar particle S which has a mass m_S and a momentum p^μ. In the CP-conserving framework, the most general coupling of S to a pair of gauge bosons and that to a pair of the Higgs bosons can be parametrized by

$$S(p)V_\mu(p_1)V'_\nu(p_2)\colon\ m_S\left[\mathcal{A}g_{\mu\nu}+\mathcal{B}\frac{p_{2\mu}p_{1\nu}}{m_S^2}\right],\qquad Shh\colon\ m_S\mathcal{C},\tag{1}$$

where $\mathcal{A}$, $\mathcal{B}$, and $\mathcal{C}$ are dimensionless.

We write the helicity amplitudes for the decay $S\to VV'$ as

$$\langle V(p_1,\lambda_1)V'(p_2,\lambda_2)|S(p)\rangle\equiv m_S\mathcal{T}_{\lambda_1\lambda_2},\tag{2}$$

where λ_1 and λ_2 are the helicities of the outgoing gauge bosons. The dimensionless amplitudes $\mathcal{T}_{\lambda_1\lambda_2}$'s are then written in terms of $\mathcal{A}$ and $\mathcal{B}$ in Eq. (1) as [65]

$$\mathcal{T}_{++}=\mathcal{T}_{--}=-\mathcal{A},\qquad \mathcal{T}_{00}=\begin{cases}\frac{m_S^2}{4m_V^2}(2\mathcal{A}+\mathcal{B})-(\mathcal{A}+\mathcal{B}), & \text{if } m_V\equiv m_{V_1}=m_{V_2}\neq 0;\\ 0, & \text{if } m_{V_1}=0 \text{ or } m_{V_2}=0,\end{cases}\tag{3}$$

and the other helicity amplitudes are zero. The partial decay rates are

$$\Gamma(S\to VV')=\frac{1}{\mathcal{S}}\frac{\beta_{VV'}}{16\pi}m_S\sum_{\lambda_1,\lambda_2}|\mathcal{T}_{\lambda_1\lambda_2}|^2,\qquad \Gamma(S\to hh)=\frac{\beta_{hh}}{32\pi}m_S|\mathcal{C}|^2,\tag{4}$$

where the symmetric factor $\mathcal{S}$ is 1/2 for two identical outgoing particles, and $\beta_{ij}=\sqrt{1-2(m_i^2+m_j^2)/m_S^2+(m_i^2-m_j^2)^2/m_S^4}$.

When a scalar particle is heavy enough, its decay into a massive gauge boson pair VV ($V = W^{\pm}, Z$) has a special feature. The condition $m_S \gg m_V$ makes $\mathcal{T}_{00}$ highly enhanced if $(2\mathcal{A} + \mathcal{B}) \neq 0$. The SM Higgs boson, if its mass is greater than $2m_V$, has

$$\mathcal{A}^{h_{\rm SM}} = \frac{2m_V^2}{vm_h}, \qquad \mathcal{B}^{h_{\rm SM}} = 0. \tag{5}$$

The partial decay rate of $h_{\rm SM} \to V_L V_L$ is proportional to the cube of m_h while that of $h_{\rm SM} \to V_T V_T$ is inversely proportional to m_h. The heavier the Higgs boson is, the more dominant $h \to V_L V_L$ will become. Since $\Gamma(h \to t\bar{t})$ is also linearly proportional to m_h, the Higgs boson decay into $V_L V_L$ is dominant. This is called the longitudinal polarization enhancement.

The partial decay rate of S into a pair of SM Higgs bosons is sizable if $\mathcal{C} \sim \mathcal{O}(1)$. In the MSSM, an obvious scalar boson candidate which decays into hh is the heavy CP-even Higgs boson H^0. However, $H^0 \to hh$ is suppressed in the alignment limit since $\mathcal{C}$ is [66]

$$\mathcal{C}^{H^0} = -\frac{3g_Z^2 \sin 4\beta}{8} \frac{v}{M_{H^0}} [1 + \mathcal{O}(\cos(\beta - \alpha))], \tag{6}$$

where $g_Z = g/\cos\theta_W$ and θ_W is the weak mixing angle. The partial decay rate $\Gamma(H^0 \to hh)$ is inversely proportional to the heavy Higgs mass: there is no enhancement in the hh decay channel.

III. MODEL WITH A SINGLET SCALAR AND VECTORLIKE QUARKS

We consider a simple extension of the SM by introducing a CP-even singlet scalar boson S_0, a VLQ doublet $\mathcal{Q}_{L/R}$, two VLQ singlets $\mathcal{U}_{L/R}$ and $\mathcal{D}_{L/R}$:

$$\mathcal{Q}_{L/R} = \begin{pmatrix} \mathcal{U}' \\ \mathcal{D}' \end{pmatrix}_{L/R}, \qquad \mathcal{U}_{L/R}, \qquad \mathcal{D}_{L/R}. \tag{7}$$

The $SU(3)_c \times SU(2)_L \times U(1)_Y$ quantum numbers of $\mathcal{Q}_{L/R}$, $\mathcal{U}_{L/R}$, $D_{L/R}$ are $(\mathbf{3}, \mathbf{2}, 1/3)$, $(\mathbf{3}, \mathbf{1}, 4/3)$, and $(\mathbf{3}, \mathbf{1}, -2/3)$, respectively. The hypercharges of VLQs are set to be the same as the SM quarks. Different assignment shall affect the decays of S into ZZ and $\gamma\gamma$.

The most general scalar potential of the SM Higgs doublet H and a real singlet scalar S_0 is [67]

$$\begin{aligned} V(H, S_0) = &-\mu^2 H^\dagger H + \lambda (H^\dagger H)^2 + \frac{a_1}{2} S_0 H^\dagger H + \frac{a_2}{2} S_0^2 H^\dagger H \\ &+ b_1 S_0 + \frac{b_2}{2} S_0^2 + \frac{b_3}{3} S_0^3 + \frac{b_4}{4} S_0^4. \end{aligned} \tag{8}$$

Note that we do not assume any discrete Z_2 symmetry for S_0. When defining the neutral component of H as $\phi_0 = (v_0 + h_0)/\sqrt{2}$ and the VEV of the singlet field as $\langle S_0 \rangle = x$, the extrema of the potential satisfy

$$\frac{\partial V(v_0/\sqrt{2}, x)}{\partial v_0} = 0, \qquad \frac{\partial V(v_0/\sqrt{2}, x)}{\partial x} = 0. \tag{9}$$

Although there exist many possible extrema, the true minimum of H should generate proper EWSB, i.e., $v = 246$ GeV. On the other hand, the VEV of S is free to choose since the shift of the singlet field, $S \to S + \Delta_S$, corresponds to redefining the parameters of $a_{1,2}$ and $b_{1,\ldots,4}$. There is no change in physics. Without loss of generality we take $(v_0, x) = (v, 0)$. Note that the choice of vanishing VEV for S_0 eliminates the tadpole term of S_0. The minimization conditions in Eq. (9) become

$$\mu^2 = \lambda v^2, \qquad b_1 = -\frac{v^2}{4} a_1. \tag{10}$$

The Yukawa terms of VLQs with the singlet S_0 and the SM Higgs doublet H as well as their mass terms are

$$\begin{aligned} -\mathcal{L}_Y = &S_0 [y_\mathcal{Q} \bar{\mathcal{Q}} \mathcal{Q} + y_\mathcal{U} \bar{\mathcal{U}} \mathcal{U} + y_\mathcal{D} \bar{\mathcal{D}} \mathcal{D}] + M_\mathcal{Q} \bar{\mathcal{Q}} \mathcal{Q} + M_\mathcal{U} \bar{\mathcal{U}} \mathcal{U} \\ &+ M_\mathcal{D} \bar{\mathcal{D}} \mathcal{D} + [Y_\mathcal{D} \bar{\mathcal{Q}}_L H \mathcal{D}_R + Y'_\mathcal{D} \bar{\mathcal{Q}}_R H \mathcal{D}_L \\ &+ Y_\mathcal{U} \bar{\mathcal{Q}}_L \tilde{H} \mathcal{U}_R + Y'_\mathcal{U} \bar{\mathcal{Q}}_R \tilde{H} \mathcal{U}_L + \text{H.c.}], \end{aligned} \tag{11}$$

where $\tilde{H} = i\tau_2 H^*$. For simplicity, we assume $y_\mathcal{Q} = y_\mathcal{U} = y_\mathcal{D} \equiv y_S$, $Y_\mathcal{U} = Y_{\mathcal{U}'}$, and $Y_\mathcal{D} = Y_{\mathcal{D}'}$ in what follows.

The VLQ mass matrix $\mathbb{M}_F$ in the basis of (F', F) where $F = \mathcal{U}, \mathcal{D}$ is

$$\mathbb{M}_F = \begin{pmatrix} M_\mathcal{Q} & \frac{Y_F v}{\sqrt{2}} \\ \frac{Y_F v}{\sqrt{2}} & M_F \end{pmatrix}, \tag{12}$$

which is diagonalized by the mixing matrix of

$$\mathbb{R}_{\theta_F} = \begin{pmatrix} c_{\theta_F} & -s_{\theta_F} \\ s_{\theta_F} & c_{\theta_F} \end{pmatrix}. \tag{13}$$

Here we adopt simplifying notations of $c_x = \cos x$ and $s_x = \sin x$. The $Y_\mathcal{U}$ and $Y_\mathcal{D}$ terms generate the mixings between VLQ doublet and VLQ singlets. If $Y_F \sim \mathcal{O}(1)$, VLQ mixing angles are small since VLQs are expected to be heavy. The mass eigenvalues and the mixing angle are then

$$\begin{aligned} M_{F_1, F_2} &= \frac{1}{2} \left[M_\mathcal{Q} + M_F \mp \sqrt{(M_F - M_\mathcal{Q})^2 + 2Y_F^2 v^2} \right], \\ s_{2\theta_F} &= \frac{\sqrt{2} Y_F v}{M_{F_2} - M_{F_1}}, \end{aligned} \tag{14}$$

where $M_{F_1} < M_{F_2}$.

The Yukawa terms of the VLQ mass eigenstates become

$$-\mathcal{L}_{\text{Yukawa}} = y_S S_0 \sum_i [\bar{\mathcal{U}}_i \mathcal{U}_i + \bar{\mathcal{D}}_i \mathcal{D}_i] + h_0 \sum_F \sum_{i,j} y_{hF_iF_j} \bar{F}_i F_j, \tag{15}$$

where $F = \mathcal{U}, \mathcal{D}$, i, $j = 1, 2$, and $y_{hF_iF_j}$ are

$$y_{hF_1F_1} = -y_{hF_2F_2} = -\frac{Y_F}{\sqrt{2}} s_{2\theta_F},$$
$$y_{hF_1F_2} = y_{hF_2F_1} = -\frac{Y_F}{\sqrt{2}} c_{2\theta_F}. \tag{16}$$

The gauge interaction Lagrangian in terms of the VLQ mass eigenstates is

$$\mathcal{L}_{\text{gauge}} = eA_\mu \sum_F \sum_i Q_F \bar{F}_i \gamma^\mu F_i + g_Z Z_\mu \sum_F \sum_{i,j} \hat{g}_{ZF_iF_j} \bar{F}_i \gamma^\mu F_j + \frac{g}{\sqrt{2}} \left[W^{+\mu} \sum_{i,j} \hat{g}_{W\mathcal{U}_i\mathcal{D}_j} \bar{\mathcal{U}}_i \gamma_\mu \mathcal{D}_j + \text{H.c.} \right]. \tag{17}$$

Here Q_F is the electric charge of the fermion F and the effective gauge couplings $\hat{g}_{VFF'}$ are

$$\hat{g}_{ZF_1F_1} = \bar{g}^v_{\mathcal{Q}} c^2_{\theta_F} + \bar{g}^v_F s^2_{\theta_F}, \qquad \hat{g}_{ZF_2F_2} = \bar{g}^v_{\mathcal{Q}} s^2_{\theta_F} + \bar{g}^v_F c^2_{\theta_F},$$
$$\hat{g}_{ZF_1F_2} = (\bar{g}^v_{\mathcal{Q}} - \bar{g}^v_F) s_{\theta_F} c_{\theta_F},$$
$$\hat{g}_{W\mathcal{U}_1\mathcal{D}_1} = c_{\theta_\mathcal{U}} c_{\theta_\mathcal{D}}, \qquad \hat{g}_{W\mathcal{U}_1\mathcal{D}_2} = c_{\theta_\mathcal{U}} s_{\theta_\mathcal{D}},$$
$$\hat{g}_{W\mathcal{U}_2\mathcal{D}_1} = s_{\theta_\mathcal{U}} c_{\theta_\mathcal{D}}, \qquad \hat{g}_{W\mathcal{U}_2\mathcal{D}_2} = s_{\theta_\mathcal{U}} s_{\theta_\mathcal{D}}, \tag{18}$$

where $\hat{g}_{VFF'} = \hat{g}_{VF'F}$ and $\bar{g}^v_{\mathcal{F}} = \frac{1}{2} T_3^{\mathcal{F}} - s^2_W Q_{\mathcal{F}}$ for $\mathcal{F} = \mathcal{Q}, \mathcal{U}, \mathcal{D}$. There is a big difference between h-F-F' couplings and V-F-F' couplings. In the limit of $\theta_{\mathcal{U},\mathcal{D}} \ll 1$, the gauge couplings to different mass eigenstates of VLQs (e.g. $\hat{g}_{VF_1F_2'}$) are suppressed by s_{θ_F}. On the contrary, the VLQ couplings to the Higgs boson are suppressed for the same mass eigenstates.

Without the Z_2 symmetry, the S_0 field can couple to the SM particles at tree level. Since the singlet scalar S_0 is neutral under all quantum numbers of the SM gauge group, the only possible renormalizable couplings of S_0 to the SM particles at tree level are to the Higgs boson through a_1 and a_2 terms in Eq. (8). However, nonzero a_1 will generate the S-h mixing at tree level. Then the Higgs coupling modifiers of κ_V and κ_f are changed into c_η, where η is the S-h mixing angle. According to the global fit analysis of the LHC Higgs precision data [68–70], c_η is very close to 1. Nonzero a_1 builds up some tension with the Higgs boson constraints. Moreover, our main question is whether the longitudinal polarization enhancement of S decay remains at loop level. Therefore, we consider a limiting scenario in which the singlet scalar has no tree-level couplings with the Higgs boson:

$$a_1^{\text{tree}} = 0 = a_2^{\text{tree}}. \tag{19}$$

IV. THE EFFECTS OF THE VLQ LOOPS

In the previous section, we suggested a rather extreme scenario where S_0 does not interact with the SM Higgs boson at tree level. The singlet field S_0 could be considered as a field in a hidden sector. In the model, the visible sector and the hidden sector are connected via VLQ loops: the VLQs play the role of messengers. There are two phenomenological implications: (i) the singlet-Higgs mixing and (ii) the radiative decays of S into SM particles. We study the effects at one loop level.

A. *S*-*h* mixing and Higgs Modifiers

First, the S-h mixing is radiatively generated through the VLQ loops as shown in Fig. 1. The scalar mass-squared matrix in the basis of (h_0, S_0) becomes

$$\mathbb{M}^2_{hS} \equiv \begin{pmatrix} 2\lambda v^2 & \delta M^2_{Sh} \\ \delta M^2_{Sh} & M^2_{SS} \end{pmatrix}, \tag{20}$$

where $M^2_{SS} = b_2$ since we have used the conditions in Eq. (10) with our choice of the vacuum $(v_0, x) = (v, 0)$. At one loop level, we have

$$\delta M^2_{Sh} = \frac{y_S N_c}{4\pi^2} \sum_F \sum_i y_{hF_iF_i} M^2_{F_i} [4(\tau^S_{F_i} - 1) g(\tau^S_{F_i}) - 4\tau^S_{F_i} + 5], \tag{21}$$

where $N_c = 3$ is the color factor of the VLQ, $F = \mathcal{U}, \mathcal{D}$, $i = 1, 2$, $\tau^i_j = m_i^2/(4m_j^2)$, and $y_{hFF'}$'s are in Eq. (16).[1] The loop function $g(\tau)$ is given by

$$g(\tau) = \begin{cases} \sqrt{\tau^{-1} - 1} \arcsin \sqrt{\tau} & \text{if } \tau \le 1; \\ \frac{\sqrt{1-\tau^{-1}}}{2} \left[\log \frac{1+\sqrt{1-\tau^{-1}}}{1-\sqrt{1-\tau^{-1}}} - i\pi \right] & \text{if } \tau > 1. \end{cases} \tag{22}$$

Note that δM^2_{Sh} vanishes if $M_{F_1} = M_{F_2}$ since $y_{hF_1F_1} = -y_{hF_2F_2}$: see Eq. (16). Significant S-h mixing requires sizable mass differences of F_1 and F_2.

[1]There is UV divergence in the one loop calculation of δM^2_{Sh} which must be properly renormalized. Detailed description on the renormalization of the whole model is in preparation [71].

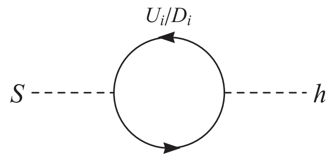

FIG. 1. Feynman diagrams for the loop-induced S-h mixing.

The mass eigenvalues and the S-h mixing angle η are

$$m_{h,S}^2 = \frac{1}{2}\left(M_{hh}^2 + M_{SS}^2 \mp \sqrt{(M_{SS}^2 - M_{hh}^2)^2 + 4(\delta M_{Sh}^2)^2}\right),$$
$$s_{2\eta} = \frac{2\delta M_{Sh}^2}{m_S^2 - m_h^2}, \tag{23}$$

where we use the S-h mixing matrix $\mathbb{R}_\eta$ in Eq. (13). Since δM_{Sh}^2 is radiatively generated, we expect $s_\eta \ll 1$. We take the mass eigenstate $h = c_\eta h_0 - s_\eta S_0$ to be the observed Higgs boson with a mass of 125 GeV, and S to be heavy such as $m_S \gtrsim 500$ GeV.

The nonzero S-h mixing changes the Higgs coupling modifiers of $\kappa_Z, \kappa_W, \kappa_t, \kappa_\tau$, and κ_b into c_η. The loop-induced decays of the Higgs boson into gg and $\gamma\gamma$ are parametrized by κ_g and κ_γ:

$$\mathcal{L}_{\rm Higgs} = \kappa_g c_g^{\rm SM}\frac{h}{v}G^{a\mu\nu}G_{\mu\nu}^a + \kappa_\gamma c_\gamma^{\rm SM}\frac{h}{v}F^{\mu\nu}F_{\mu\nu}. \tag{24}$$

The SM values $c_g^{\rm SM}$ and $c_\gamma^{\rm SM}$ are

$$c_g^{\rm SM} \equiv \frac{\alpha_s}{16\pi}A_{hgg}^{\rm SM}, \qquad c_\gamma^{\rm SM} \equiv \frac{\alpha_e}{8\pi}A_{h\gamma\gamma}^{\rm SM}, \tag{25}$$

where $A_{hgg}^{\rm SM} = \sum_{f=t,b}A_{1/2}(\tau_f^h)$, $A_{h\gamma\gamma}^{\rm SM} = A_1(\tau_W^h) + \sum_{f=t,b,\tau}N_C^f Q_f^2 A_{1/2}(\tau_f^h)$, and $A_{1/2}(\tau)$ and $A_1(\tau)$ are referred to Ref. [72]. The modifiers κ_g and κ_γ receive two kinds of new contributions. One is from the modified couplings of h to the SM particles through the S-h mixing. The other is from the triangle VLQ loops:

$$\mathcal{A}_{hgg}^{\rm VLQ} = \sum_F\sum_i y_{hF_iF_i}\frac{v}{M_{F_i}}A_{1/2}(\tau_{F_i}^h),$$
$$\mathcal{A}_{h\gamma\gamma}^{\rm VLQ} = \sum_F\sum_i N_C Q_{F_i}^2 y_{hF_iF_i}\frac{v}{M_{F_i}}A_{1/2}(\tau_{F_i}^h), \tag{26}$$

where $F = \mathcal{U}, \mathcal{D}$, $i = 1, 2$, $\tau_j^i = m_i^2/(4m_j^2)$. Then κ_g and κ_γ are

$$\kappa_{g,\gamma} = \frac{c_\eta A_{hgg,h\gamma\gamma}^{\rm SM} + \mathcal{A}_{hgg,h\gamma\gamma}^{\rm VLQ}}{A_{hgg,h\gamma\gamma}^{\rm SM}}. \tag{27}$$

Since $y_{hF_1F_1}$ and $y_{hF_2F_2}$ in Eq. (16) have opposite signs, both δM_{Sh}^2 as well as $\mathcal{A}_{hgg,h\gamma\gamma}^{\rm VLQ}$ are suppressed when $M_{F_1} \simeq M_{F_2}$.

Brief comments on strong first order electroweak phase transition are in order here. The main reason why a singlet scalar model can easily accommodate strong first order phase transition is the extended scalar field space to earn more freedom. Naturally the mixing between S and the Higgs boson is essential to enjoy the extended scalar field space. In Ref. [58], the extensive parameter scan showed that strong first order electroweak phase transition requires nonzero a_1 of the order of 100 GeV. Since a_1 vanishes at tree level in our limit scenario, the critical question is whether the loop-induced $a_1^{\rm loop}$ can be about 100 GeV. We find that this happens when there are sizable mass differences between VLQs: for example, $\Delta M_{F_1F_2} \sim 100$ GeV yields $a_1^{\rm loop} \sim \mathcal{O}(100)$ GeV. As shall be shown, $\Delta M_{F_1F_2} \sim 100$ GeV is still allowed by the current experimental results. In summary, our limiting scenario can provide a strong first order electroweak phase transition.

B. Radiative decays of S

Another important effect of the VLQ loops is the radiative decay of S into the SM particles, which occurs through the S-h mixing as in Fig. 1 and/or through the triangle VLQ loops into a gauge boson pair or a Higgs boson pair as in Fig. 2. Since we consider the case of $m_S \gtrsim 500$ GeV, the main decay modes are into $t\bar{t}$, gg, $\gamma\gamma$, WW, ZZ, and hh.

The decay of S into a top quark pair is only through the S-h mixing. The partial decay rate is

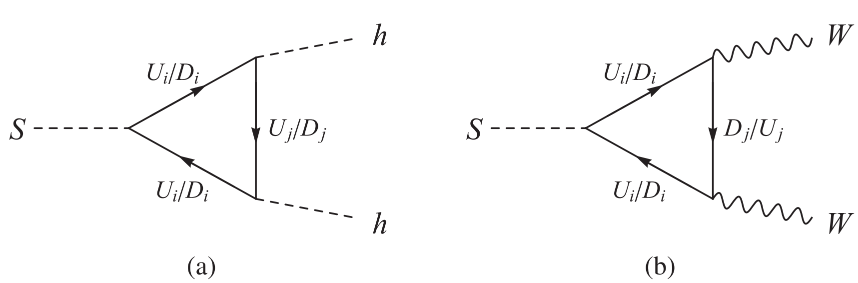

FIG. 2. Feynman diagrams of $S \to hh$ and $S \to WW$ from the VLQ loops.

$$\Gamma(S \to t\bar{t}) = s_\eta^2 \Gamma(h_{\rm SM} \to t\bar{t})|_{m_{h_{\rm SM}}=m_S}. \tag{28}$$

Another important decay channel is $S \to hh$ shown in Fig. 2(a). The vertex $\mathcal{C}$ in Eq. (1) at one loop level is

$$\mathcal{C} = \frac{y_S N_c}{4\pi^2} \sum_F \sum_{i,j} y_{hF_iF_j}^2 \mathcal{C}_T(m_h, m_S, M_{F_i}, M_{F_j}) + \frac{3m_h^2}{v m_S} s_\eta, \tag{29}$$

where $y_{hFF'}$ are given in Eq. (16). The first term is due to the triangle diagrams while the second one is from the S-h mixing. The asymptotic expression[2] of $\mathcal{C}_T(m_h, m_S, M_{F_i}, M_{F_j})$ when $m_h \ll m_S$ and $\Delta_F \ll M_\mathcal{F}$, where $\Delta_F = M_{F_j} - M_{F_i}$ and $M_\mathcal{F} = (M_{F_i} + M_{F_j})/2$, is very useful to understand the enhancement of $\Gamma(S \to hh)$ in some parameter space,

$$\sqrt{\tau}\mathcal{C}_T = 2 + (1 - 2\tau^{-1}) f(\tau) - 2g(\tau) + \left(\frac{\Delta_F^2}{M_\mathcal{F}^2}\right)\left[\frac{8\tau^2 + 49\tau - 48}{12\tau(1-\tau)} + \frac{(\tau^3 + 12\tau^2 - 26\tau + 16)g(\tau)}{4\tau(1-\tau)^2}\right] + \left(\frac{m_h^2}{m_S^2}\right)\left[\frac{2(6-\tau)}{3} + \frac{2(\tau-2)f(\tau)}{\tau}\right] + \mathcal{O}\left(\frac{\Delta_F^4}{M_\mathcal{F}^4}\right) + \mathcal{O}\left(\frac{m_h^4}{m_S^4}\right), \tag{30}$$

where $\tau = m_S^2/(4M_\mathcal{F}^2)$ and $f(\tau)$ is referred to Ref. [72]. Note that the odd power terms in $(\Delta_F/M_\mathcal{F})$ are neglected since they cancel each other after the summation in Eq. (29). If y_S, $Y_{\mathcal{U},\mathcal{D}} \sim \mathcal{O}(1)$, $\mathcal{C}$ is not suppressed by large m_S, contrary to the case of a heavy CP-even scalar H^0 of the MSSM in Eq. (6). Another important result is that the partial decay rate $\Gamma(S \to hh)$ increases with Δ_F, the mass difference between M_{F_i} and M_{F_j}. Since Δ_F is proportional to the Higgs VEV from the SM-like Yukawa couplings of the VLQs to the Higgs boson, the enhancement of $S \to hh$ can be considered as nondecoupling effects.

The VLQ loops also allow the decay of S into a massive gauge boson pair VV ($V = W, Z$) as shown in Fig. 2(b). The dimensionless parameters $\mathcal{A}$ and $\mathcal{B}$ in Eq. (1) are

$$\begin{aligned}
\mathcal{A}_{WW} &= \frac{g^2 y_S N_c}{8\pi^2} \sum_{i,j} [\hat{g}_{W\mathcal{U}_i\mathcal{D}_j}^2 \mathcal{A}_T(m_W, m_S, M_{\mathcal{U}_i}, M_{\mathcal{D}_j}) + \{\mathcal{U} \leftrightarrow \mathcal{D}\}] + \frac{2m_W^2}{v m_S} s_\eta, \\
\mathcal{B}_{WW} &= \frac{g^2 y_S N_c}{8\pi^2} \sum_{i,j} [\hat{g}_{W\mathcal{U}_i\mathcal{D}_j}^2 \mathcal{B}_T(m_W, m_S, M_{\mathcal{U}_i}, M_{\mathcal{D}_j}) + \{\mathcal{U} \leftrightarrow \mathcal{D}\}], \\
\mathcal{A}_{ZZ} &= \frac{g_Z^2 y_S N_c}{4\pi^2} \sum_{i,j} [\hat{g}_{Z\mathcal{U}_i\mathcal{U}_j}^2 \mathcal{A}_T(m_Z, m_S, M_{\mathcal{U}_i}, M_{\mathcal{U}_j}) + \{\mathcal{U} \leftrightarrow \mathcal{D}\}] + \frac{2m_Z^2}{v m_S} s_\eta, \\
\mathcal{B}_{ZZ} &= \frac{g_Z^2 y_S N_c}{4\pi^2} \sum_{i,j} [\hat{g}_{Z\mathcal{U}_i\mathcal{U}_j}^2 \mathcal{B}_T(m_Z, m_S, M_{\mathcal{U}_i}, M_{\mathcal{U}_j}) + \{\mathcal{U} \leftrightarrow \mathcal{D}\}],
\end{aligned} \tag{31}$$

where $i, j = 1, 2$. $\mathcal{A}_{VV}$ consists of two parts, one from the triangle VLQ loops and the other from the S-h mixing, while $\mathcal{B}_{VV}$ is only from the triangle loops.

Our main question is whether the longitudinal polarization enhancement in $S \to VV$ remains significant at loop level, which happens when $2\mathcal{A} + \mathcal{B} \neq 0$ as shown in Eq. (3). The S-h-mixing-induced terms, proportional to s_η in Eq. (31), appear only in $\mathcal{A}$ and thus generate the longitudinal polarization enhancement. The condition that the triangle VLQ loops induce the enhancement is easy to see through the asymptotic behaviors of $\mathcal{A}_T$ and $\mathcal{B}_T$ in the limit of $\Delta_F \ll M_\mathcal{F}$ and $m_V \ll m_S$, given by

$$\sqrt{\tau}\mathcal{A}_T = 1 + (1 - \tau^{-1}) f(\tau) + \left(\frac{\Delta_F^2}{M^2}\right)\left[-\frac{1}{4} + \frac{(3\tau - 4)f(\tau)}{4\tau^2} + \frac{(\tau^2 + 4\tau - 8)g(\tau)}{4\tau(\tau - 1)}\right] + 2\left(\frac{m_V^2}{m_S^2}\right)[3 - \tau - \tau^{-1} f(\tau) - 2g(\tau)] + \mathcal{O}\left(\frac{\Delta_F^4}{M^4}\right) + \mathcal{O}\left(\frac{m_V^4}{m_S^4}\right), \tag{32}$$

$$\sqrt{\tau}\mathcal{B}_T = -2 - 2(1-\tau^{-1})f(\tau) + \left(\frac{\Delta_F^2}{M^2}\right)\left[\frac{5}{2} + \frac{(8-5\tau)f(\tau)}{2\tau^2} - \frac{(\tau^2+12\tau-16)g(\tau)}{2\tau(\tau-1)}\right] + 4\left(\frac{m_V^2}{m_S^2}\right)[\tau - 4 + (2-\tau)\tau^{-1}f(\tau) + 2g(\tau)] + \mathcal{O}\left(\frac{\Delta_F^4}{M^4}\right) + \mathcal{O}\left(\frac{m_V^4}{m_S^4}\right), \quad (33)$$

where $\tau = m_S^2/(4M_\mathcal{F}^2)$. Equations (33) and (33) show that $2\mathcal{A} + \mathcal{B} \sim \mathcal{O}(m_V^2/m_S^2)$ if $\Delta_F = 0$. Sizable mass differences of VLQs are crucial for the longitudinal polarization enhancement through the triangle VLQ loops.

The last category of the radiative decays of S is into gg, $\gamma\gamma$, and $Z\gamma$. When at least one of the outgoing gauge bosons is massless, there is no longitudinal polarization mode as shown in Eq. (3). The $\mathcal{A}$'s are

$$\mathcal{A}_{\gamma\gamma} = \frac{e^2 y_S N_c}{4\pi^2}\sum_F\sum_i Q_{F_i}^2 \frac{1}{\sqrt{\tau_{F_i}}}[1 + (1-\tau_{F_i}^{-1})f(\tau_{F_i})],$$

$$\mathcal{A}_{gg} = \delta^{ab}\frac{g_s^2 y_S}{8\pi^2}\sum_F\sum_i \frac{1}{\sqrt{\tau_{F_i}}}[1 + (1-\tau_{F_i}^{-1})f(\tau_{F_i})],$$

$$\mathcal{A}_{Z\gamma} = \frac{e g_Z y_S N_c}{2\pi^2}\sum_F\sum_i Q_{F_i}\hat{g}_{ZF_iF_i} \times \frac{1}{\sqrt{\tau_{F_i}}}\left[-1 - (1-\tau_{F_i}^{-1})f(\tau_{F_i}) + \mathcal{O}\left(\frac{m_Z^2}{m_S^2}\right)\right], \quad (34)$$

where a, b are color indices of the outgoing gluons, $F = \mathcal{U}, \mathcal{D}$, $i = 1$, 2, and $\tau_{F_i} = m_S^2/(4M_{F_i}^2)$. The $\mathcal{B}$'s can be obtained by using Ward identity as follows:

$$\mathcal{B}_{\gamma\gamma} = -2\mathcal{A}_{\gamma\gamma}, \qquad \mathcal{B}_{gg} = -2\mathcal{A}_{gg},$$

$$\mathcal{B}_{Z\gamma} = -2\left(1 - \frac{m_Z^2}{m_S^2}\right)^{-1}\mathcal{A}_{Z\gamma}. \quad (35)$$

The final comment in this section is the importance of introducing three VLQ multiplets. If we introduce only one VLQ multiplet, there is no Yukawa couplings with the *Higgs boson*: the S-h mixing and the $S \to hh$ decay will be absent. In addition, the VLQs running in the triangle VLQ loops for the decay of $S \to WW, ZZ$ have the same masses because of no VLQ mixing. There will be no longitudinal polarization enhancement and thus the signal rates of the radiative decays shall have typical loop suppression [73]. In summary, the presence of the VLQ doublet *and* the VLQ singlets are crucial for the enhanced radiative decays of S.

V. NUMERICAL RESULTS

The phenomenological characteristics of the singlet scalar S depend on the model parameters of y_S, m_S, $Y_{\mathcal{U},\mathcal{D}}$, $M_\mathcal{Q}$, $M_\mathcal{U}$ and $M_\mathcal{D}$. The y_S contributes equally to all of the partial decay rates of S by the common factor of y_S^2 since S decays only radiatively through VLQ loops in our model. The branching ratios of S are independent of y_S. The m_S dependence on the branching ratios is also weak for the heavy S. The $Y_{\mathcal{U},\mathcal{D}}$, $M_\mathcal{Q}$, and $M_{\mathcal{U},\mathcal{D}}$ specify the VLQ mass matrices and thus the mass difference Δ_F. Since $Y_\mathcal{U}$ and $Y_\mathcal{D}$ also quantify the VLQ couplings with the Higgs boson, they are the most crucial parameters.

Therefore, we consider a simple benchmark parameter line, given by

$$M_\mathcal{Q} = M_\mathcal{U} = M_\mathcal{D}, \qquad Y_\mathcal{U} = 0, Y_\mathcal{D} \text{ varies.} \quad (36)$$

We found that the results in this simple case display the main characteristic features of the radiative decays of S. The VLQ mass spectra become

$$M_{\mathcal{U}_1} = M_{\mathcal{U}_2} = M_\mathcal{Q}, \qquad M_{\mathcal{D}_{1,2}} = M_\mathcal{Q} \mp \frac{1}{\sqrt{2}}|Y_\mathcal{D}|v. \quad (37)$$

Note that $\mathcal{D}_1$ becomes the lightest VLQ and $\Delta M_{\mathcal{U}_1\mathcal{D}_1} = \Delta M_{\mathcal{D}_2\mathcal{U}_1} = (1/2)\Delta M_{\mathcal{D}_2\mathcal{D}_1}$ where $\Delta M_{ij} \equiv M_i - M_j$. Our setting of $Y_\mathcal{U} \neq Y_\mathcal{D}$ generates a sizable mass difference $\Delta M_{\mathcal{U}_1\mathcal{D}_1}$ which is essential for the longitudinal polarization enhancement of $S \to WW$.

Brief comments on the VLQ masses are in order here. The mass bounds on the VLQs from the direct searches at the Tevatron and the LHC depend sensitively on the decay channels of the VLQs. If the main decay mode includes the third generation quarks, the bounds are strong: $M_{\text{VLQ}} \gtrsim$ 400–600 GeV [74–77]. If VLQs mix only with lighter generations, the mass bounds become much less than 400 GeV [74], which is adopted here.

In Fig. 3, we present the branching ratios of the singlet scalar S as functions of $\Delta M_{\mathcal{U}_1\mathcal{D}_1}$, or equivalently of $Y_\mathcal{D}$, along the benchmark parameter line. We consider two cases, $m_S = 500$ GeV and $m_S = 750$ GeV with $M_{\mathcal{D}_1} = 0.6 m_S$. When $Y_\mathcal{D} = 0$ ($Y_\mathcal{U} = 0$ by setting), the dominant decay mode is into gg with almost 100% branching ratio. The radiative decay of S into hh is certainly prohibited. In addition there is no radiatively generated S-h mixing, i.e., $s_\eta = 0$, which forbids the decay of $S \to t\bar{t}$. The mixing-induced decays in $S \to WW, ZZ$ are closed and only the triangle VLQ loop contributions become relevant. The next dominant decay mode is into WW with very small branching ratio of the order of 10^{-3}. This is because of the suppression of the longitudinal polarization enhancement since the $Y_\mathcal{D} = 0$ condition makes all of the VLQ masses degenerate and thus $2\mathcal{A} + \mathcal{B} \sim \mathcal{O}(m_V^2/m_S^2)$: see

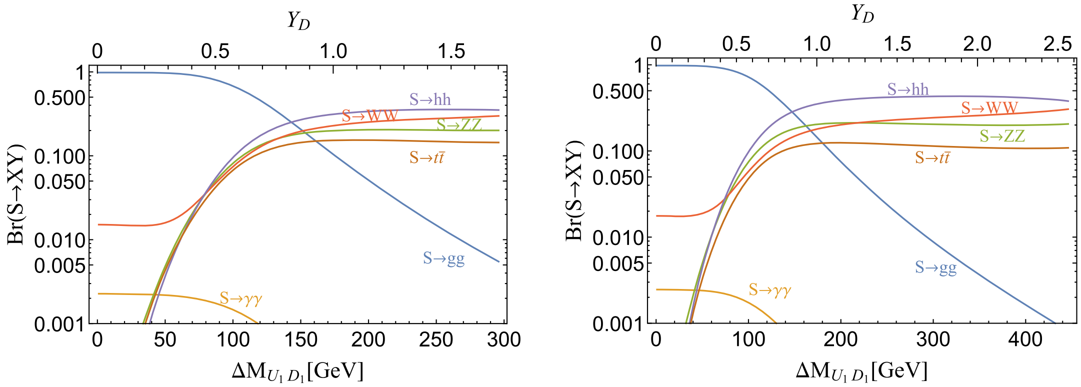

(a) $m_S = 500$ GeV (b) $m_S = 750$ GeV

FIG. 3. Branching ratios of the singlet scalar S with mass $m_S = 500, 750$ GeV as functions of $\Delta M_{\mathcal{U}_1\mathcal{D}_1} (\equiv M_{\mathcal{U}_1} - M_{\mathcal{D}_1})$. For the VLQ masses we set the lightest VLQ mass as $M_{\mathcal{D}_1} = 0.6 m_S$ and assume $M_{\mathcal{Q}} = M_{\mathcal{U}} = M_{\mathcal{D}}$ and $Y_{\mathcal{U}} = 0$ with varying $Y_{\mathcal{D}}$.

Eqs. (30), (32), and (33). The reason why $\mathrm{B}(S \to WW)$ is much larger than $\mathrm{B}(S \to ZZ)$ when $Y_{\mathcal{U},\mathcal{D}} = 0$ is that the gauge couplings of VLQs to the Z boson are smaller than those to the W boson with our choice of the electric charges of VLQs. Note that $\Gamma(S \to WW) \gg \Gamma(S \to \gamma\gamma, ZZ)$ is generic in the view of high dimensional operators in the effective field theory [78].

As $Y_{\mathcal{D}}$ increases, the decay modes into hh, WW, ZZ and $t\bar{t}$ all become significant. For both $m_S = 500$ GeV and $m_S = 750$ GeV cases, the hh mode is as important as the gg mode when $Y_{\mathcal{D}} \simeq 0.8$, and dominant when $Y_{\mathcal{D}} \gtrsim 0.9$, followed by the WW, ZZ, and $t\bar{t}$ modes. We found that the little hierarchy among hh, WW, ZZ and $t\bar{t}$ modes is quite generic with more general parameter setup. In some extreme corners of the parameter space such as small $Y_{\mathcal{U},\mathcal{D}}$ but large Δ_F, the WW decay mode is dominant.

In Fig. 4, we show the total decay rate of S as a function of $\Delta M_{\mathcal{U}_1\mathcal{D}_1}$ for $m_S = 500$ GeV and $m_S = 750$ GeV. When $\Delta M_{\mathcal{U}_1\mathcal{D}_1} = 0$, $\Gamma_S^{\mathrm{tot}} \sim 0.1$ GeV for both mass cases. The singlet scalar is a very narrow resonance. With increasing $\Delta M_{\mathcal{U}_1\mathcal{D}_1}$, Γ_S^{tot} starts decreasing, which is expected since $\mathcal{U}_{1,2}$ and $\mathcal{D}_2$ become heavier with the fixed $M_{\mathcal{D}_1}$ and thus make smaller loop corrections. When $\Delta M_{\mathcal{U}_1\mathcal{D}_1}$ is large enough, however, Γ_S^{tot} turns to increase, reaching about 10 GeV when $\Delta M_{\mathcal{U}_1\mathcal{D}_1} = 300$ GeV. The enhancement compared to the $\Delta M_{\mathcal{U}_1\mathcal{D}_1} = 0$ case is almost by two orders of magnitude. This is unexpected since the VLQ masses for $\Delta M_{\mathcal{U}_1\mathcal{D}_1} = 300$ GeV are much heavier than those for $\Delta M_{\mathcal{U}_1\mathcal{D}_1} = 0$. This shows how dramatic the enhancement of the radiative decays of S can be when there exist sizable mass differences of the VLQs.

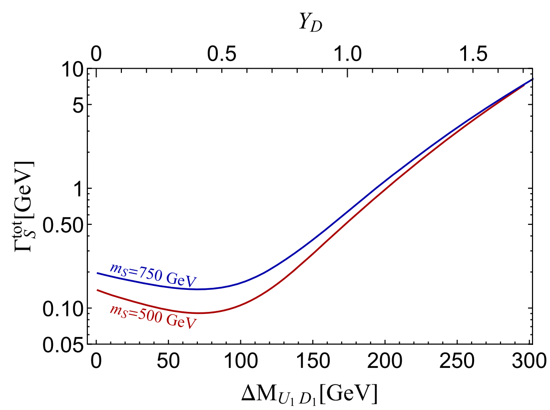

FIG. 4. Total decay rate of the singlet scalar S as a function of $\Delta M_{\mathcal{U}_1\mathcal{D}_1}$ or $Y_{\mathcal{D}}$ for $m_S = 500$ GeV and $m_S = 750$ GeV. We take the benchmark parameter line in Eq. (36).

Figure 5 presents the 95% C.L. exclusion region in the $(\Delta M_{\mathcal{U}_1\mathcal{D}_1}, y_S)$ parameter plane by the LHC Higgs precision data as well as the heavy Higgs search results in the WW, ZZ, and hh channels. We also show the contours for s_η by dashed (orange) lines. For the Higgs precision data, we adopt the global fit results from the ATLAS/CMS combined analysis for $\kappa_V \le 1$ [70]: $\kappa_V = 0.97 \pm 0.060$, $\kappa_g = 0.81^{+0.13}_{-0.10}$, and $\kappa_\gamma = 0.90^{+0.10}_{-0.09}$. Note that $\kappa_\tau = 0.87^{+0.12}_{-0.11}$ and $\kappa_b = 0.57^{+0.16}_{-0.16}$ are consistent within 2σ but $\kappa_t = 1.42^{+0.23}_{-0.22}$ shows some deviation. For heavy scalar boson searches with mass $m_S = 500$ (750) GeV, the observed 95% C.L. upper bounds on $\sigma \cdot \mathrm{B}$ at $\sqrt{s} = 8$ TeV are 200 fb (40 fb) for WW [79,80], 43 fb (12 fb) for ZZ [81], and 107.6 fb (34 fb) for hh [82–84]. We found that the heavy scalar search channels of dijet [85,86] and $W\gamma/Z\gamma$ [87] provide weaker constraints. We do not consider the $t\bar{t}$ channel [88,89] because the current bound ignores the interference with the continuum background, which can be very significant [90–92].

The Higgs precision data exclude large $\Delta M_{\mathcal{U}_1\mathcal{D}_1}$, almost independently of y_S: $\Delta M_{\mathcal{U}_1\mathcal{D}_1} \lesssim 200\,(300)$ GeV for $m_S = 500\,(750)$ GeV is allowed. This exclusion mainly comes from the constraint on κ_g. When $\Delta M_{\mathcal{U}_1\mathcal{D}_1}$ is small, or equivalently when all of the VLQ masses are almost degenerate, the opposite signs between $y_{hF_1F_1}$ and $y_{hF_2F_2}$

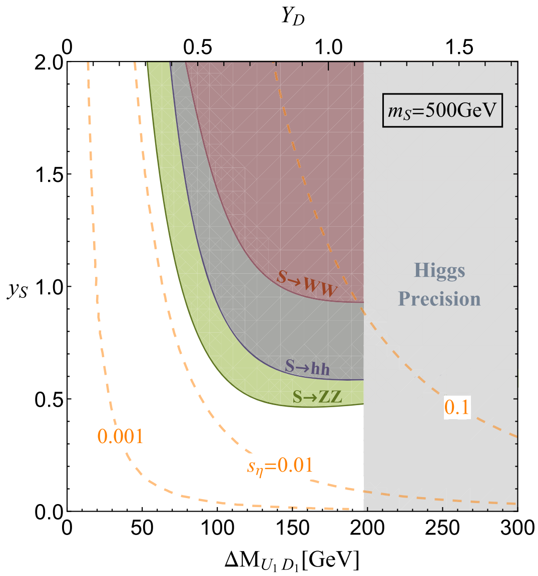

(a) $m_S = 500$ GeV

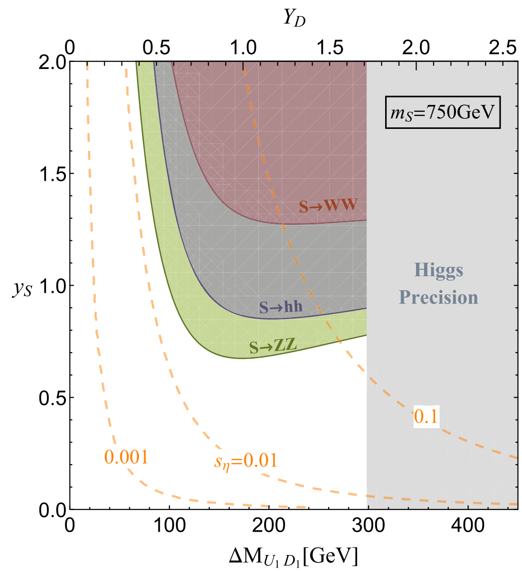

(b) $m_S = 750$ GeV

FIG. 5. The constraints in the parameter space of $(\Delta M_{\mathcal{U}_1\mathcal{D}_1}, y_S)$ from the current LHC Higgs data as well as the $\sqrt{s} = 8$ TeV searches for a heavy Higgs decaying into WW, ZZ, and hh: (a) is for $m_S = 500$ GeV and (b) is for $m_S = 750$ GeV.

cause significant cancellation of the F_1 and F_2 contributions. Therefore, κ_g is within the allowed value. As the VLQ mass difference increases, the VLQ loop corrections become more important. The Higgs precision data put an upper bound on $\Delta M_{\mathcal{U}_1\mathcal{D}_1}$. The κ_γ is less sensitive since the dominant contribution to κ_γ comes from the W loop. The S-h mixing effect, mainly on κ_V, is minor since we adopt the Higgs precision data at 2σ level such that $s_\eta \lesssim 0.5$ [69].

Figure 5 shows that the ZZ channel in the heavy scalar searches puts the strongest bound for both mass cases. This is attributed to compatible branching ratios of WW, hh, and ZZ modes but much smaller LHC upper bounds on $\sigma \cdot \mathrm{B}$ for the ZZ mode because of its clean signal. The parameter space with large y_S and large $Y_\mathcal{D}$ is excluded. We also present the contours of s_η by dashed (orange) lines. It is clear to see that the current heavy Higgs searches put stronger bounds on the S-h mixing angle than the Higgs precision data. In most parameter space, s_η should be less than about 0.01 (0.05) for $m_S = 500\,(750)$ GeV. The radiatively generated S-h mixing is significantly constrained by the current LHC data.

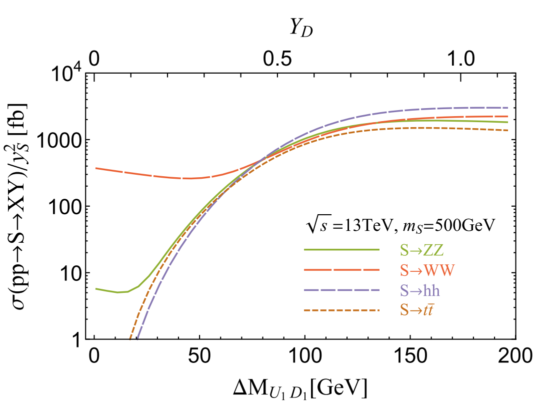

FIG. 6. Cross sections of production and decay of S for the main decay channels with $m_S = 500$ GeV and $\sqrt{s} = 13$ TeV at the LHC. The cross sections are normalized by y_S^2.

Finally, we show in Fig. 6 the cross section times branching ratio $\sigma(pp \to S) \times B(S \to XY)$ as a function of $\Delta M_{\mathcal{U}_1\mathcal{D}_1}$ with $m_S = 500$ GeV at the 13 TeV LHC. The decay of S into gg is not considered because of the overwhelming QCD background. We normalize $\sigma \cdot \mathrm{B}$ by y_S^2. Incorporating the current Higgs precision constraint on $\Delta M_{\mathcal{U}_1\mathcal{D}_1}$, we present the results for $\Delta M_{\mathcal{U}_1\mathcal{D}_1}$ up to 200 GeV. In the whole parameter space, the WW mode is leading or next-to-leading, having $\sigma \cdot \mathrm{B} \sim \mathcal{O}(100\text{–}1000)$ fb. The cleanest search mode, the ZZ one, also has sizable signal rate about 100 fb if $\Delta M_{\mathcal{U}_1\mathcal{D}_1} \gtrsim 50$ GeV. The hh channel is also promising with sufficient VLQ mass differences.

VI. CONCLUSIONS

In a simple extension of the SM with an additional singlet scalar field S, we answer the question whether a unique feature of a heavy scalar boson, the longitudinal polarization enhancement in its decay into a massive gauge boson pair, remains at loop level. In order to focus on the loop-induced effects, we consider a limiting scenario where S does not interact with the SM Higgs boson at tree level. Since S decouples from the SM world at tree level, we introduced vectorlike quarks (VLQs) as messengers between S and the

SM particles. In order for the Higgs boson to interact also with the VLQs, one VLQ doublet and two VLQ singlets are suggested. There are two up-type VLQs and two down-type VLQs, $\mathcal{U}_{1,2}$ and $\mathcal{D}_{1,2}$. Through the Yukawa couplings of VLQs with S and the Higgs boson, the VLQs generate radiatively the S-h mixing as well as the decays of S into gg, WW, ZZ, and hh.

We found that the most required condition for enhancing the radiative decay rates of S into WW, ZZ, and hh is the large mass differences of VLQs. This is contrary to the common expectation since large mass differences with the fixed lightest VLQ mass mean heavy VLQs and thus smaller loop corrections. First the radiatively generated S-h mixing is proportional to the coupling of h-F_i-F_i ($F = \mathcal{U}, \mathcal{D}$ and $i = 1, 2$). When $M_{F_1} = M_{F_2}$, the opposite signs between h-F_1-F_1 and h-F_2-F_2 couplings cancel the contributions of F_1 and F_2. As $\Delta M_{F_2F_1} (\equiv M_{F_2} - M_{F_1})$ increases, the S-h mixing is enhanced. The mixing-induced decays of S into WW, ZZ, hh, and $t\bar{t}$ become significant. Another kind of the VLQ contribution to the radiative decay of S is through the triangle VLQ loops. We showed that the longitudinal polarization enhancement in $S \to WW, ZZ$ through the triangular VLQ loops happens also when the mass differences of the VLQs become large.

In order to illustrate the phenomenological features, we considered a simple benchmark scenario where $Y_\mathcal{D}$ controls the VLQ mass differences with the fixed lightest VLQ mass. Two cases of $m_S = 500$ GeV and $m_S = 750$ GeV are studied. When $\Delta M_{FF'} = 0$, both the S-h mixing and the longitudinal polarization enhancement in $S \to VV$ vanish, which makes $S \to gg$ dominant. The total decay rate is of the order of 0.1 GeV for $m_S \sim 500$ GeV. If $\Delta M_{FF'}$ is sizable such as $Y_\mathcal{D} \simeq 0.8$, the decay of S into hh becomes as important as that into gg. For $Y_\mathcal{D} \gtrsim 0.8$, $\mathrm{B}(S \to gg)$ drops rapidly, and the decays into hh, WW, ZZ, and $t\bar{t}$ become similarly dominant. The enhancement of the total decay rate of S is high, by one order of magnitude when $Y_\mathcal{D} = 1$. This is contrary to the naive prediction that heavier VLQs running in the loop would cause smaller loop corrections.

We also presented the 95% C.L. exclusion regions of $(Y_\mathcal{D}, y_S)$ from the current LHC bounds including the Higgs precision data and the heavy scalar searches in the channel of WW, ZZ, and hh. Among various Higgs precision data, κ_g puts the strongest upper bound on $Y_\mathcal{D}$: $Y_\mathcal{D} \lesssim 1.1$ for $m_S = 500$ GeV and $Y_\mathcal{D} \lesssim 1.7$ for $m_S = 750$ GeV. The heavy scalar searches also put additional constraints. In particular, the ZZ channel data severely limit the S-h mixing angle η, more than the Higgs precision data: $s_\eta \lesssim 0.05$ for $m_S = 500$ GeV and $s_\eta \lesssim 0.1$ for $m_S = 750$ GeV are allowed. In conclusions, our loop calculation in a UV model with a singlet scalar and three VLQ multiplets shows that the radiative decays of S can be very enhanced when the mass spectrum of the VLQs shows diversity. Note that the presence of multiple VLQs is crucial for the enhanced radiative decays of S since sizable mass differences among VLQs are required. Therefore, the persistent searches for a heavy scalar boson at the future LHC are of great importance in constraining new particles that appear at loop level.

ACKNOWLEDGMENTS

K. C. was supported by the MoST of Taiwan under Grants No. MOST-105-2112-M-007-028-MY3. S. K. was supported by the National Research Foundation of Korea, Grant No. 2015R1D1A1A01058726. The work of J. S. and Y. W. Y. was supported by the National Research Foundation of Korea, Grant No. NRF-2016R1D1A1B03932102.

[1] K. Kowalska, Eur. Phys. J. C **76**, 684 (2016).
[2] B. Patt and F. Wilczek, arXiv:hep-ph/0605188.
[3] M. J. Strassler and K. M. Zurek, Phys. Lett. B **651**, 374 (2007).
[4] C. Englert, T. Plehn, D. Zerwas, and P. M. Zerwas, Phys. Lett. B **703**, 298 (2011).
[5] R. N. Cahn and S. Dawson, Phys. Lett. B **136**, 196 (1984); **138**, 464(E) (1984).
[6] G. L. Kane, W. W. Repko, and W. B. Rolnick, Phys. Lett. B **148**, 367 (1984).
[7] R. Schabinger and J. D. Wells, Phys. Rev. D **72**, 093007 (2005).
[8] J. Ellis, S. A. R. Ellis, J. Quevillon, V. Sanz, and T. You, J. High Energy Phys. 03 (2016) 176.
[9] V. Barger, P. Langacker, M. McCaskey, M. J. Ramsey-Musolf, and G. Shaughnessy, Phys. Rev. D **77**, 035005 (2008).
[10] S. Dawson and W. Yan, Phys. Rev. D **79**, 095002 (2009).
[11] P. J. Fox, D. Tucker-Smith, and N. Weiner, J. High Energy Phys. 06 (2011) 127.
[12] B. Batell, S. Gori, and L. T. Wang, J. High Energy Phys. 06 (2012) 172.
[13] D. Bertolini and M. McCullough, J. High Energy Phys. 12 (2012) 118.
[14] T. Robens and T. Stefaniak, Eur. Phys. J. C **75**, 104 (2015).
[15] K. Fuyuto and E. Senaha, Phys. Rev. D **90**, 015015 (2014).
[16] V. A. Kuzmin, V. A. Rubakov, and M. E. Shaposhnikov, Phys. Lett. **155B**, 36 (1985).
[17] A. I. Bochkarev and M. E. Shaposhnikov, Mod. Phys. Lett. A **02**, 417 (1987).
[18] J. Choi and R. R. Volkas, Phys. Lett. B **317**, 385 (1993).
[19] J. M. Cline and P. A. Lemieux, Phys. Rev. D **55**, 3873 (1997).

[20] S. W. Ham, Y. S. Jeong, and S. K. Oh, J. Phys. G **31**, 857 (2005).
[21] A. Ahriche, Phys. Rev. D **75**, 083522 (2007).
[22] S. Profumo, M. J. Ramsey-Musolf, and G. Shaughnessy, J. High Eenrgy Phys. **08** (2007) 010.
[23] J. R. Espinosa, T. Konstandin, and F. Riva, Nucl. Phys. **B854**, 592 (2012).
[24] T. Li and Y. F. Zhou, J. High Energy Phys. 07 (2014) 006.
[25] S. Profumo, M. J. Ramsey-Musolf, C. L. Wainwright, and P. Winslow, Phys. Rev. D **91**, 035018 (2015).
[26] M. Kamionkowski, A. Kosowsky, and M. S. Turner, Phys. Rev. D **49**, 2837 (1994).
[27] S. J. Huber and T. Konstandin, J. Cosmol. Astropart. Phys. 09 (2008) 022.
[28] J. R. Espinosa, T. Konstandin, J. M. No, and G. Servant, J. Cosmol. Astropart. Phys. 06 (2010) 028.
[29] J. M. No, Phys. Rev. D **84**, 124025 (2011).
[30] M. Hindmarsh, S. J. Huber, K. Rummukainen, and D. J. Weir, Phys. Rev. Lett. **112**, 041301 (2014).
[31] M. Hindmarsh, S. J. Huber, K. Rummukainen, and D. J. Weir, Phys. Rev. D **92**, 123009 (2015).
[32] C. Caprini *et al.*, J. Cosmol. Astropart. Phys. 04 (2016) 001.
[33] K. Hashino, M. Kakizaki, S. Kanemura, and T. Matsui, Phys. Rev. D **94**, 015005 (2016).
[34] L. Leitao, A. Megevand, and A. D. Sanchez, J. Cosmol. Astropart. Phys. 10 (2012) 024.
[35] Y. Kikuta, K. Kohri, and E. So, arXiv:1405.4166.
[36] R. Jinno, K. Nakayama, and M. Takimoto, Phys. Rev. D **93**, 045024 (2016).
[37] L. Leitao and A. Megevand, J. Cosmol. Astropart. Phys. 05 (2016) 037.
[38] J. Jaeckel, V. V. Khoze, and M. Spannowsky, Phys. Rev. D **94**, 103519 (2016).
[39] P. S. B. Dev and A. Mazumdar, Phys. Rev. D **93**, 104001 (2016).
[40] L. Lavoura and J. P. Silva, Phys. Rev. D **47**, 2046 (1993).
[41] J. A. Aguilar-Saavedra, R. Benbrik, S. Heinemeyer, and M. Perez-Victoria, Phys. Rev. D **88**, 094010 (2013).
[42] B. A. Dobrescu and C. T. Hill, Phys. Rev. Lett. **81**, 2634 (1998).
[43] R. S. Chivukula, B. A. Dobrescu, H. Georgi, and C. T. Hill, Phys. Rev. D **59**, 075003 (1999).
[44] L. Randall and R. Sundrum, Phys. Rev. Lett. **83**, 3370 (1999).
[45] T. Appelquist, H. C. Cheng, and B. A. Dobrescu, Phys. Rev. D **64**, 035002 (2001).
[46] N. Arkani-Hamed, A. G. Cohen, E. Katz, and A. E. Nelson, J. High Energy Phys. 07 (2002) 034.
[47] T. Han, H. E. Logan, B. McElrath, and L. T. Wang, Phys. Rev. D **67**, 095004 (2003).
[48] M. Perelstein, M. E. Peskin, and A. Pierce, Phys. Rev. D **69**, 075002 (2004).
[49] T. Moroi and Y. Okada, Mod. Phys. Lett. A **07**, 187 (1992).
[50] K. S. Babu, I. Gogoladze, M. U. Rehman, and Q. Shafi, Phys. Rev. D **78**, 055017 (2008).
[51] S. P. Martin, Phys. Rev. D **81**, 035004 (2010).
[52] P. W. Graham, A. Ismail, S. Rajendran, and P. Saraswat, Phys. Rev. D **81**, 055016 (2010).
[53] C. Anastasiou, S. Buehler, E. Furlan, F. Herzog, and A. Lazopoulos, Phys. Lett. B **702**, 224 (2011).
[54] O. Eberhardt, G. Herbert, H. Lacker, A. Lenz, A. Menzel, U. Nierste, and M. Wiebusch, Phys. Rev. Lett. **109**, 241802 (2012).
[55] C. Anastasiou, C. Duhr, F. Dulat, E. Furlan, T. Gehrmann, F. Herzog, A. Lazopoulos, and B. Mistlberger, J. High Energy Phys. 05 (2016) 058.
[56] G. Cynolter and E. Lendvai, Eur. Phys. J. C **58**, 463 (2008).
[57] J. Cao, Y. He, P. Wu, M. Zhang, and J. Zhu, J. High Energy Phys. 01 (2014) 150.
[58] M. L. Xiao and J. H. Yu, Phys. Rev. D **90**, 014007 (2014); **90**, 019901 (2014).
[59] B. Batell, S. Jung, and H. M. Lee, J. High Energy Phys. 01 (2013) 135.
[60] G. Degrassi, S. Di Vita, J. Elias-Miro, J. R. Espinosa, G. F. Giudice, G. Isidori, and A. Strumia, J. High Energy Phys. 08 (2012) 098.
[61] D. Buttazzo, G. Degrassi, P. P. Giardino, G. F. Giudice, F. Sala, A. Salvio, and A. Strumia, J. High Energy Phys. 12 (2013) 089.
[62] D. F. Litim, M. Mojaza, and F. Sannino, J. High Energy Phys. 01 (2016) 081.
[63] G. M. Pelaggi, F. Sannino, A. Strumia, and E. Vigiani, arXiv:1701.01453.
[64] M. L. Xiao and J. H. Yu, Phys. Rev. D **94**, 015011 (2016).
[65] S. Y. Choi, D. J. Miller, M. M. Muhlleitner, and P. M. Zerwas, Phys. Lett. B **553**, 61 (2003).
[66] N. Craig, J. Galloway, and S. Thomas, arXiv:1305.2424.
[67] C. Y. Chen, S. Dawson, and I. M. Lewis, Phys. Rev. D **91**, 035015 (2015).
[68] M. J. Dolan, J. L. Hewett, M. Krmer, and T. G. Rizzo, J. High Energy Phys. 07 (2016) 039.
[69] K. Cheung, P. Ko, J. S. Lee, and P. Y. Tseng, J. High Energy Phys. 10 (2015) 057.
[70] ATLAS and CMS Collaborations, Report No. ATLAS-CONF-2015-044.
[71] S. K. Kang, Jeonghyeon Song, and Y. W. Yoon (to be published).
[72] A. Djouadi, Phys. Rep. **457**, 1 (2008).
[73] Q. H. Cao, C. B. Jackson, W. Y. Keung, I. Low, and J. Shu, Phys. Rev. D **81**, 015010 (2010).
[74] Y. Okada and L. Panizzi, Adv. High Energy Phys. **2013**, 1 (2013).
[75] ATLAS Collaboration, Report No. ATLAS-CONF-2016-020.
[76] ATLAS Collaboration, Report No. ATLAS-CONF-2017-015.
[77] CMS Collaboration, Report No. CMS-PAS-B2G-17-007.
[78] R. Franceschini, G. F. Giudice, J. F. Kamenik, M. McCullough, A. Pomarol, R. Rattazzi, M. Redi, F. Riva, A. Strumia, and R. Torre, J. High Energy Phys. 03 (2016) 144.
[79] G. Aad *et al.* (ATLAS Collaboration), J. High Energy Phys. 01 (2016) 032.
[80] V. Khachatryan *et al.* (CMS Collaboration), J. High Energy Phys. 10 (2015) 144.
[81] G. Aad *et al.* (ATLAS Collaboration), Eur. Phys. J. C **76**, 45 (2016).
[82] G. Aad *et al.* (ATLAS Collaboration), Phys. Rev. Lett. **114**, 081802 (2015).
[83] G. Aad *et al.* (ATLAS Collaboration), Eur. Phys. J. C **75**, 412 (2015).

[84] G. Aad *et al.* (ATLAS Collaboration), Phys. Rev. D **92**, 092004 (2015).
[85] G. Aad *et al.* (ATLAS Collaboration), Phys. Rev. D **91**, 052007 (2015).
[86] CMS Collaboration, Report No. CMS-PAS-EXO-14-005.
[87] G. Aad *et al.* (ATLAS Collaboration), Phys. Lett. B **738**, 428 (2014).
[88] G. Aad *et al.* (ATLAS Collaboration), J. High Energy Phys. 08 (2015) 148.
[89] V. Khachatryan *et al.* (CMS Collaboration), Phys. Rev. D **93**, 012001 (2016).
[90] S. Jung, J. Song, and Y. W. Yoon, Phys. Rev. D **92**, 055009 (2015).
[91] M. Carena and Z. Liu, J. High Energy Phys. 11 (2016) 159.
[92] R. Barcelo and M. Masip, Phys. Rev. D **81**, 075019 (2010).